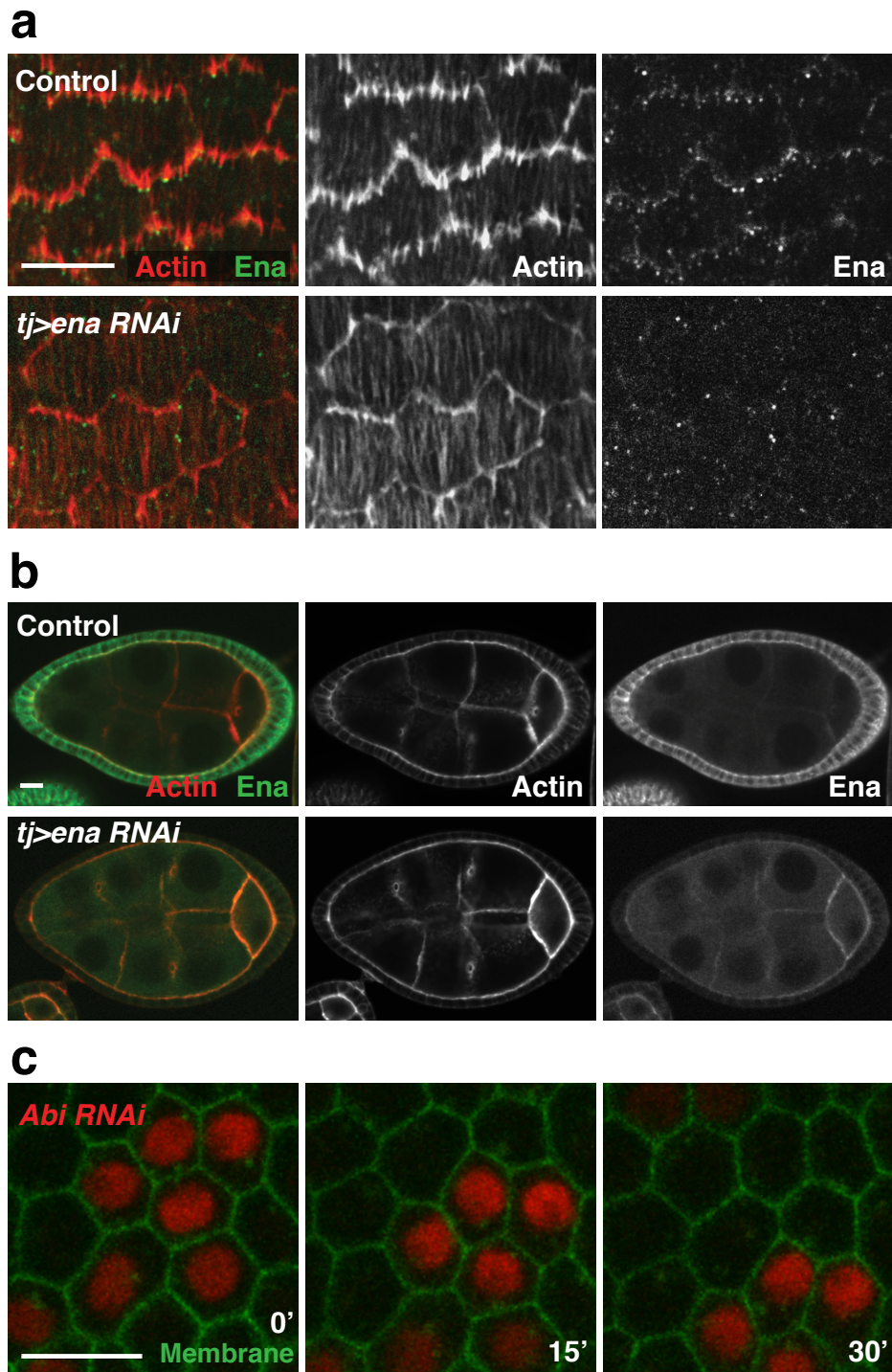
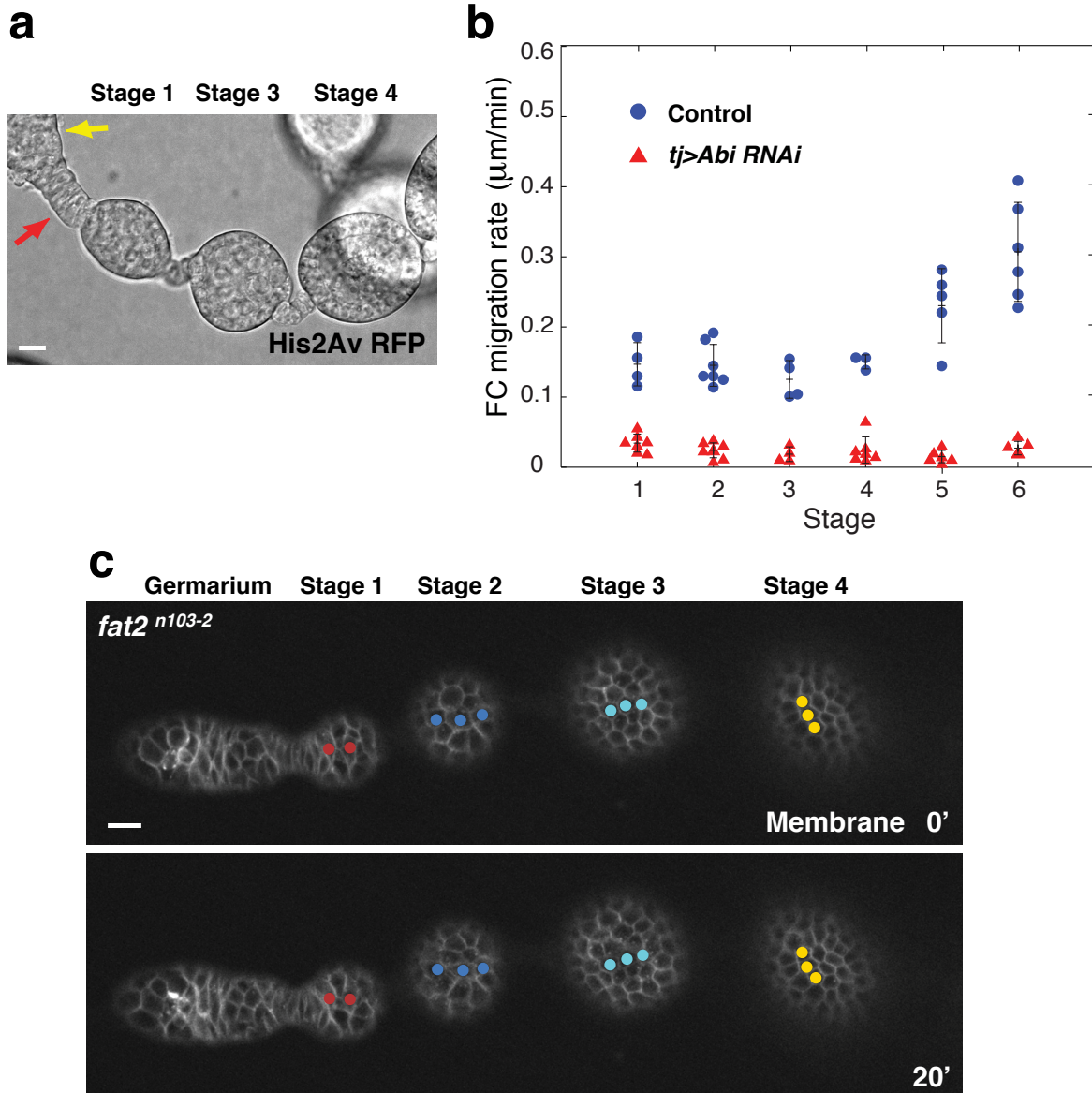


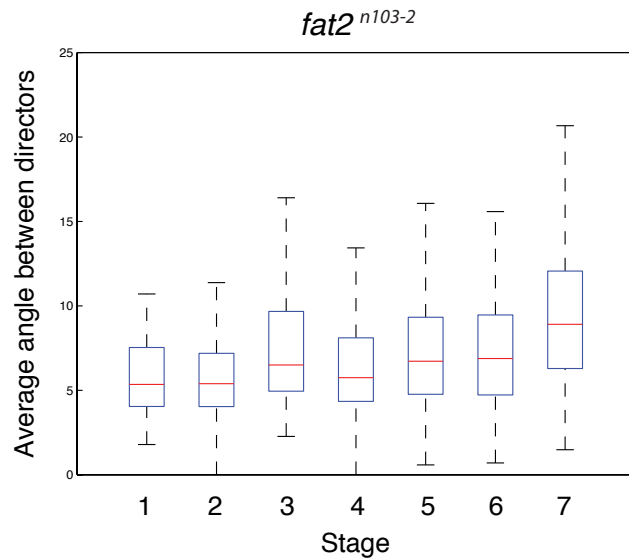
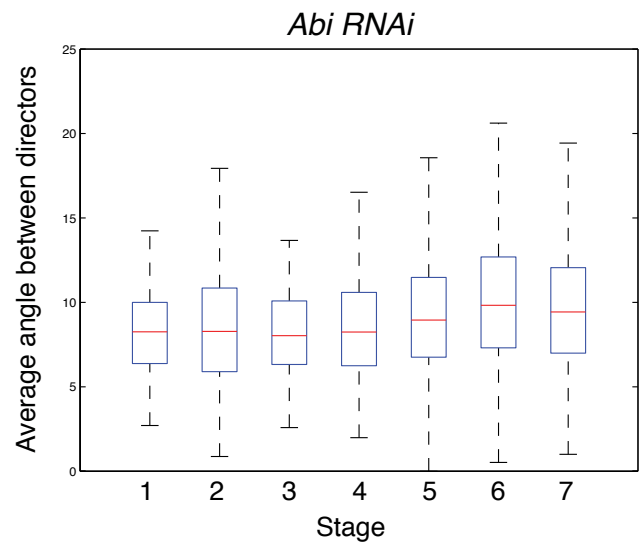
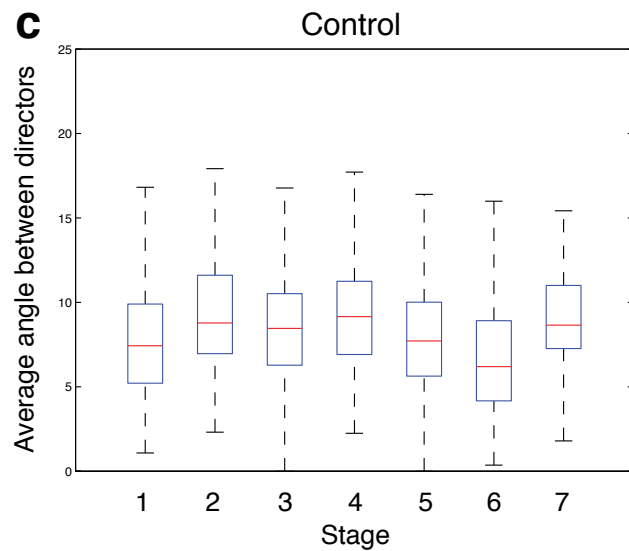
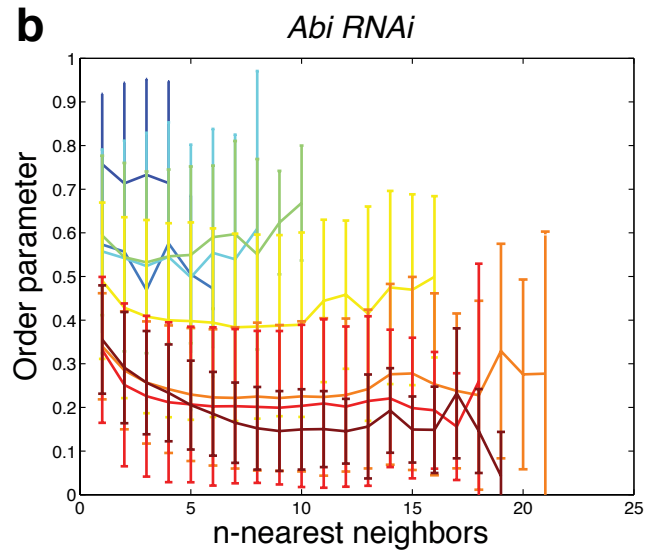
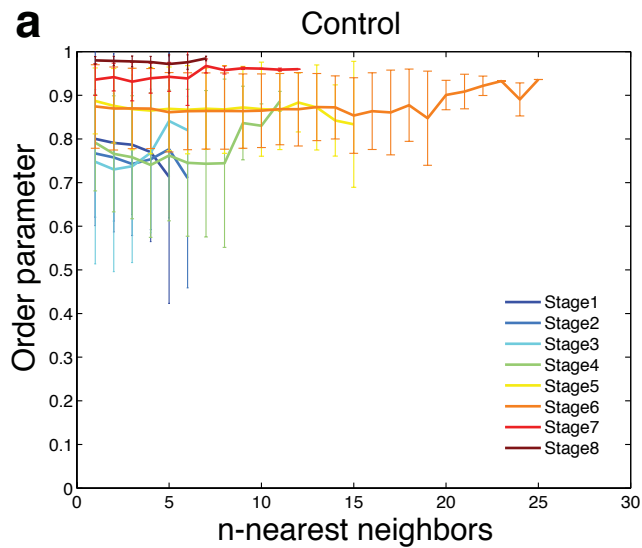
Supplementary Figure 1 The leading edge actin networks are distinct from the basal actin bundles. Laser-scanning confocal images were taken at the basal epithelial surface of stage seven and eight egg chambers. Scale bars, 10 μm. (a) Clonal expression of *ena RNAi* (green) reduces filopodia compared to adjacent wild-type cells. (b) SCAR is still present at the leading edges of the follicle cells in the absence of filopodia under *ena RNAi* conditions. (c) Ena does not localize to the leading edge when protrusions are eliminated in clones expressing *Abi RNAi* (green). (d-e) The regulatory chain of non-muscle Myosin II (Spaghetti Squash mCherry) (d), and the focal adhesion component Paxillin (Pax GFP) (e) are both localized along the basal actin bundles. (f) Protrusions can extend orthogonally to the basal bundles in wild-type cells of a *msn*¹⁰² mosaic egg chamber (arrow). Ena marks the tips of filopodia.



Supplementary Figure 2 The role of filopodia and lamellipodia in egg chamber rotation. *ena RNAi* was expressed in all follicle cells with the *tj-Gal4* driver. **(a)** *ena RNAi* eliminates filopodia and localization of Ena at the leading edge of the follicle cells. **(b)** A transverse section of an egg chamber expressing *tj-Gal4>ena RNAi* shows a strong loss of Ena protein in the follicle cells. **(c)** A small clone expressing *Abi RNAi* is carried along within the migrating epithelium. The follicle cell membranes of a stage seven egg chamber are marked with the Nrg GFP protein trap. Follicle cells expressing *Abi RNAi* are marked with RFP. Spinning disk confocal images of stage seven egg chambers. Scale bars, 10 μ m.



Supplementary Figure 3 Early egg chamber rotation requires lamellipodia and Fat2. (a) A transverse section through the three egg chambers shown in Fig. 4b and Supplemental Video 4. The stage one egg chamber is connected to the germarium (yellow arrow) by a double-layered stalk (red arrow). Bright field image. Scale bar, 10 μm . (b) Live imaging was used to determine the contributions of lamellipodia (*Abi*) during early rotation stages. Expressing *Abi RNAi* in all follicle cells (FC) throughout oogenesis with the *traffic jam-Gal4* (*tj-Gal4*) driver blocks the rotation of stage one-six egg chambers. Individual data points, mean \pm SEM, t-test: $***P < 3.20 \times 10^{-4}$ for all stages. (c) A *fat2* ovariolar region containing stage one, two, three and four egg chambers that do not rotate during a twenty minute time series. Colored dots indicate a row of cells at 0 and 20 minutes. FM4-64 dye was used to label cell membranes. We were unable to detect rotation in four *fat2* ovariolar regions containing a total of 10 egg chambers between stages one and five. Spinning disk confocal images. Scale bar, 10 μm .



Supplementary Figure 4 Control data for tissue- and cell-level actin bundle alignment in rotating and non-rotating egg chambers. **(a,b)** Average order parameter during rotation stages for control **(a)** and *Abi RNAi* **(b)** epithelia as a function of the size of the epithelial region analyzed. The size of each region is varied from adjacent neighbors to n -connected regions. We observe no dependence of the average order parameter on the size of the region analyzed. **(c)** Actin bundle alignment within individual follicle cells throughout development in control, *Abi RNAi* and *fat2ⁿ¹⁰³⁻²* egg chambers. Box plots show the median standard deviation of the angles between directors in an individual follicle cell. Basal actin bundles within each cell remain aligned in *Abi RNAi* and *fat2ⁿ¹⁰³⁻²* conditions.

Supplementary Figure 5 Rotation is specifically required to maintain tissue-level actin bundle alignment during early stages. (a) The *mirr-Gal4* driver begins expressing weakly in the central region of the follicle cell epithelium at stage six (not shown). By stage eight, it drives strong expression of *UAS-RFP* in the same region. Laser-scanning confocal images. (b) *mirr-Gal4* driving *Abi RNAi* with one copy of SCAR removed does not reduce the follicle cell (FC) migration rate at stage six compared to controls. In the same background at stage eight, 70% of the egg chambers have stopped rotating. Individual data points, mean \pm SEM, t-test: *** $P=1.2 \times 10^{-4}$. (c) Stills from a time series of a stage seven egg chamber expressing *Utrophin::GFP*. Follicle cell migration has been blocked using the Arp2/3 inhibitor, CK-666. Leading edge protrusions disappear, but the global actin bundle pattern is normal. Laser-scanning confocal images. (d) Representative images of basement membrane polarity at different stages (Col IV, *Vkg* GFP). The basement membrane is segmented into overlapping windows and directors (green lines), which were obtained to calculate the order parameter (*S*) as described in the methods. Spinning disk confocal images. (e) A graph showing the average order parameter for Col IV in the basement membrane for stages one through eight. The value increases over time. For stages 1-5 $n \geq 6$, stages 6-8 $n \geq 10$. Data represent mean \pm SEM, t-test: * $P=0.033$, ** $P=0.003$. (f) The average order parameter for Col IV in the basement membrane is not changed by the one hour treatment with the control molecule or the Arp2/3 inhibitor. For stage 1 $n \geq 2$, stages 2-5 $n \geq 6$, stages 6-7 $n \geq 10$, stage 8 $n \geq 4$. Data points represent mean \pm SD. A t-test revealed no significant change between either of the drug treated samples when compared to the untreated condition. Scale bar, 10 μm .

Supplementary Table 1a Experimental Genotypes

Figure	Panel	Genotype	
1	C	<i>w</i> ¹¹¹⁸	
		<i>vkg-GFP</i>	
2	A	<i>hsFLP/+ ; Act5c>>Gal4, UAS-GFP/ UAS-MoeABD::mCherry</i>	
	B	<i>nrg-GFP/+ ; indy-GFP/ sqh-sqh::mCherry</i>	
	C, D	<i>w</i> ¹¹¹⁸	
	E	<i>SCAR^{Δ37}, FRT40/ ubi-eGFP, FRT40; GR1-Gal4, UAS-FLP/+</i>	
	F	<i>hsFLP/+; Act5c>>Gal4, UAS-GFP/ UAS-Abi-RNAi^{9749R-3}</i>	
3	A	<i>nrg-GFP/+ ; tj-Gal4/+ ; indy-GFP/+</i>	
		<i>nrg-GFP/+ ; tj-Gal4/ UAS-ena-RNAi^{v43058}; indy-GFP/+</i>	
		<i>nrg-GFP/+ ; tj-Gal4/+ ; UAS-Abi-RNAi^{9749R-3}/ indy-GFP</i>	
	B	<i>tj-Gal4, vkg-GFP/+</i>	
		<i>tj-Gal4, vkg-GFP/ UAS-ena-RNAi^{v43058}</i>	
		<i>tj-Gal4, vkg-GFP/+ ; UAS-Abi-RNAi^{9749R-3}/ +</i>	
	C	<i>tj-Gal4, vkg-GFP/+</i>	
		<i>tj-Gal4, vkg-GFP/+ ; UAS-Abi-RNAi^{9749R-3}/ +</i>	
	D	<i>tj-Gal4/+</i>	
		<i>tj-Gal4/+ ; UAS-Abi-RNAi^{9749R-3}/ +</i>	
	4	A	<i>w</i> ¹¹¹⁸
		B, C	<i>His2Av-mRFP</i>
5	A-D	<i>nrg-GFP/+ ; tj-Gal4/+ ; indy-GFP/+</i>	
6	A, B	<i>nrg-GFP/+ ; tj-Gal4/+ ; indy-GFP/+</i>	
		<i>nrg-GFP/+ ; tj-Gal4/+ ; indy-GFP/ UAS-Abi-RNAi^{9749R-3}</i>	
	C	<i>w</i> ¹¹¹⁸	
		<i>fat2ⁿ¹⁰³⁻²/ fat2ⁿ¹⁰³⁻²</i>	
	D	<i>nrg-GFP/+ ; tj-Gal4/+ ; indy-GFP/+</i>	
		<i>nrg-GFP/+ ; tj-Gal4/+ ; indy-GFP/ UAS-Abi-RNAi^{9749R-3}</i>	
		<i>w</i> ¹¹¹⁸	
			<i>fat2ⁿ¹⁰³⁻²/ fat2ⁿ¹⁰³⁻²</i>
E		<i>tj-Gal4/ UAS-UtrophinABD::GFP</i>	
7	A	<i>SCAR^{Δ37}/ mirr-Gal4</i>	
		<i>SCAR^{Δ37}/ mirr-Gal4; UAS-Abi-RNAi^{9749R-3}/ +</i>	
	B	<i>indy-GFP</i>	
C-F	<i>vkg-GFP</i>		
Sup.1	A	<i>hsFLP/+ ; UAS-ena-RNAi^{v43058}/ + ; Act5c>>Gal4, UAS-GFP/+</i>	
	B	<i>tj-Gal4/ UAS-ena-RNAi^{v43058}</i>	

	C	<i>hsFLP/+; Act5c>>Gal4, UAS-GFP/ UAS-Abi-RNAI^{9749R-3}</i>
	D	<i>sqh^{AX3}/ +; sqh-sqh::mCherry/ +</i>
	E	<i>tj-Gal4/ +; UAS-paxillin::GFP/ +</i>
	F	<i>e22c-GAL4, UAS-FLP/ +; msn¹⁰², FRT80/ ubi-eGFP, FRT80</i>
Sup. 2	A-C	<i>tj-Gal4/ +</i>
		<i>tj-Gal4/ UAS-ena-RNAI^{v43058}</i>
		<i>hsFLP/ nrg-GFP; Act5c>>Gal4, UAS-RFP/ UAS-Abi-RNAI^{9749R-3}</i>
Sup. 3	A	<i>His2Av-mRFP</i>
	B	<i>tj-Gal4/ +</i>
		<i>tj-Gal4/ +; UAS-Abi-RNAI^{9749R-3}/ +</i>
C	<i>fat2ⁿ¹⁰³⁻²/ fat2ⁿ¹⁰³⁻²</i>	
Sup. 4	A	<i>nrg-GFP/ +; tj-Gal4/ +; indy-GFP/ +</i>
	B	<i>nrg-GFP/ +; tj-Gal4/ +; indy-GFP/ UAS-Abi-RNAI^{9749R-3}</i>
	C	<i>nrg-GFP/ +; tj-Gal4/ +; indy-GFP/ +</i>
		<i>nrg-GFP/ +; tj-Gal4/ +; indy-GFP/ UAS-Abi-RNAI^{9749R-3}</i>
		<i>fat2ⁿ¹⁰³⁻²/ fat2ⁿ¹⁰³⁻²</i>
Sup. 5	A	<i>mirr-Gal4/ UAS-RFP</i>
	B	<i>SCAR^{Δ37}/ mirr-Gal4</i>
		<i>SCAR^{Δ37}/ mirr-Gal4; UAS-Abi-RNAI^{9749R-3}/ +</i>
	C	<i>tj-Gal4/ UAS-UtrophinABD::GFP</i>
	D-F	<i>vkg-GFP</i>

Supplementary Table 1b Experimental Genotypes

Movie	Genotype
1	<i>nrg-GFP/ +; indy-GFP/ sqh-sqh::mCherry</i>
2	<i>nrg-GFP/ +; tj-Gal4/ +; indy-GFP/ +</i>
	<i>nrg-GFP/ +; tj-Gal4/ +; indy-GFP/ UAS-Abi-RNAI^{9749R-3}</i>
3	<i>hsFLP/ nrg-GFP; Act5c>>Gal4, UAS-RFP/ UAS-Abi-RNAI^{9749R-3}</i>
4	<i>His2Av-mRFP</i>
5	<i>fat2ⁿ¹⁰³⁻²/ fat2ⁿ¹⁰³⁻²</i>
6	<i>tj-Gal4/ UAS-UtrophinABD::GFP</i>
7	<i>indy-GFP</i>
8	<i>tj-Gal4/ UAS-UtrophinABD::GFP</i>

Supplementary Table 2

Exact n values for graphs where independent data points are not shown

Figure	Stage	Experimental condition		
		Control	<i>Abi RNAi</i>	<i>ena RNAi</i>
3b	4	10	7	6
	5	15	10	13
	6	14	14	6
	7	18	9	9
	8	23	8	13
	9	15	7	11
	10	20	17	22
	11	7	3	7
	12	9	3	6
	13	6	7	8
	14	25	27	28
6b	Stage	Control	<i>Abi RNAi</i>	
	1	12	8	
	2	14	9	
	3	14	8	
	4	16	14	
	5	19	20	
	6	12	14	
	7	6	5	
8	7	4		
6c	Stage	<i>Wild-type</i>	<i>fat2ⁿ¹⁰³⁻²</i>	
	1	4	5	
	2	7	12	
	3	9	7	
	4	9	13	
	5	14	10	
	6	11	5	
	7	8	8	
8	5	4		
7d,f Sup. 5e,f	Stage	<i>Vkg GFP</i>	<i>Vkg GFP+</i> Control	<i>Vkg GFP+</i> Arp2/3 inhibitor
	1	6	2	10
	2	8	6	9
	3	7	8	14
	4	7	16	15
	5	7	24	16
	6	12	21	10
	7	14	16	15
8	10	4	4	

Supplementary Table 3 Exact n values for graphs in Supplementary Fig.4

Figure	n-nearest neighbors	Stage							
		1	2	3	4	5	6	7	8
Sup. 4a	1	12	14	14	16	19	12	6	7
	2	12	14	14	16	19	12	6	7
	3	12	14	14	16	19	12	6	7
	4	12	14	13	16	19	12	6	7
	5	8	13	11	16	19	11	6	6
	6	-	11	10	14	19	11	6	6
	7	-	-	-	12	19	11	5	3
	8	-	-	-	9	19	11	2	-
	9	-	-	-	7	19	11	2	-
	10	-	-	-	4	19	11	2	-
	11	-	-	-	-	19	11	2	-
	12	-	-	-	-	15	11	1	-
	13	-	-	-	-	12	11	-	-
	14	-	-	-	-	5	11	-	-
	15	-	-	-	-	2	10	-	-
	16	-	-	-	-	-	8	-	-
	17	-	-	-	-	-	7	-	-
	18	-	-	-	-	-	5	-	-
	19	-	-	-	-	-	4	-	-
	20	-	-	-	-	-	2	-	-
	21	-	-	-	-	-	2	-	-
	22	-	-	-	-	-	2	-	-
	23	-	-	-	-	-	1	-	-
	24	-	-	-	-	-	2	-	-
	25	-	-	-	-	-	1	-	-
Figure	n-nearest neighbors	Stage							
Sup. 4b	1	8	9	8	14	20	14	5	4
	2	8	9	8	14	20	14	5	4
	3	7	8	7	14	20	14	5	4
	4	6	9	6	14	20	14	5	4
	5	-	8	6	14	20	14	5	4
	6	-	5	6	13	20	14	5	4
	7	-	-	6	13	19	14	5	4
	8	-	-	4	11	19	14	5	4
	9	-	-	-	9	19	14	5	4
	10	-	-	-	7	19	14	5	4
	11	-	-	-	-	17	14	5	4
	12	-	-	-	-	14	14	5	4

	13	-	-	-	-	13	14	5	4
	14	-	-	-	-	10	13	5	4
	15	-	-	-	-	6	12	5	4
	16	-	-	-	-	3	11	5	4
	17	-	-	-	-	-	10	5	4
	18	-	-	-	-	-	9	5	4
	19	-	-	-	-	-	6	-	3
	20	-	-	-	-	-	5	-	-
	21	-	-	-	-	-	5	-	-
Figure	n-cells analyzed	Stage							
		1	2	3	4	5	6	7	
Sup. 4c	Control	126	256	274	548	1135	1276	174	
	<i>Abi RNAi</i>	65	103	125	451	1285	1691	588	
	<i>fat2ⁿ¹⁰³⁻²</i>	34	125	147	562	1691	430	749	